

Full Paper

Design, Synthesis, Biological Evaluation and Binding Mode Modeling of Benzimidazole Derivatives Targeting the Cannabinoid Receptor Type 1

Christian Espinosa-Bustos¹, Carlos F. Lagos², Javier Romero-Parra¹, Ana M. Zárate¹, Jaime Mella-Raipán³, Hernán Pessoa-Mahana⁴, Gonzalo Recabarren-Gajardo¹, Patricio Iturriaga-Vásquez⁵, Ricardo A. Tapia⁶, and C. David Pessoa-Mahana¹

¹ Department of Pharmacy, Faculty of Chemistry, Pontificia Universidad Católica de Chile, Santiago, Chile

² Department of Endocrinology, School of Medicine, Pontificia Universidad Católica de Chile, Santiago, Chile

³ Institute of Chemistry and Biochemistry, Faculty of Science, Universidad de Valparaíso, Playa Ancha, Valparaíso, Chile

⁴ Department of Organic and Physical Chemistry, Faculty of Chemical and Pharmaceutical Sciences, Universidad de Chile, Santiago, Chile

⁵ Department of Chemistry, Faculty of Sciences, Universidad de Chile, Santiago, Chile

⁶ Department of Organic Chemistry, Faculty of Chemistry, Pontificia Universidad Católica de Chile, Santiago, Chile

A series of *N*-acyl-2,5-dimethoxyphenyl-1*H*-benzimidazoles were designed based on a CoMFA model for cannabinoid receptor type 1 (CB1) ligands. Compounds were synthesized and radioligand binding affinity assays were performed. Eight novel benzimidazoles exhibited affinity for the CB1 receptor in the nanomolar range, and the most promising derivative compound **5** displayed a K_i value of 1.2 nM when compared to CP55,940. These results confirm our previously reported QSAR model on benzimidazole derivatives, providing new information for the development of small molecules with high CB1 affinity.

Keywords: Benzimidazole derivatives / Binding affinity / Cannabinoid receptor type 1 / CoMFA / Molecular modeling

Received: May 19, 2014; Revised: October 26, 2014; Accepted: October 30, 2014

DOI 10.1002/ardp.201400201



Additional supporting information may be found in the online version of this article at the publisher's web-site.

Introduction

Although the use of the marijuana plant (*Cannabis sativa*) for medicinal purposes has been ongoing for over 5000 years, the discovery of cannabinoid receptors and their endogenous ligands took place only two decades ago [1]. The endocannabinoid system appears to be involved in a rising number of pathological conditions and hence represents an exciting target for drug discovery [2]. This system is comprised of several endogenous ligands (anandamide, 2-arachidonoyl glycerol (2-AG), 2-arachidonoyl glyceryl ether and virodh-

amine, as well as the biological properties associated with the endocannabinoids ligands that are mainly mediated by two G-protein-coupled receptors, CB1 and CB2 [3]. The CB1 receptor is widely expressed in the central nervous system, while the CB2 receptor is mainly expressed in the spleen and the immune system [4].

Therapeutic applications of the CB1 receptor agonists have been reported for treating pain, multiple sclerosis, anxiety/mood disorders, seizures and neuroprotection [5]. On the other hand, several CB1 antagonists and inverse agonists have been evaluated for obesity, metabolic disorders, smoking cessation and alcohol abuse [6]. So far, more than five structurally diverse families of cannabinergic ligands have been discovered, including classical cannabinoids, non-classical cannabinoids, aminoalkylindoles, eicosanoids and arylpyrazoles [7]. Among these families, several indoles such as JWH-015, JWH-007 and AM-679 with CB1 receptor agonist properties have been described and more recently we have

Correspondence: Dr. C. David Pessoa-Mahana, Department of Pharmacy, Faculty of Chemistry, Pontificia Universidad Católica de Chile, Av. Vicuña Mackenna 4860, Macul 7820436, Santiago, Chile.
E-mail: cpessoa@uc.cl
Fax: +56 2 6854 744

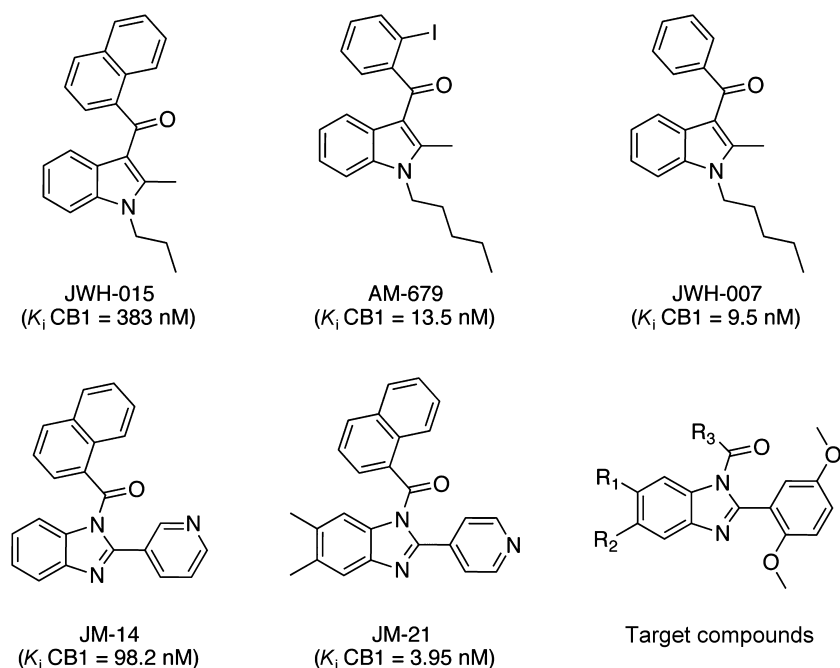


Figure 1. Chemical structures of reported indole/benzimidazole-based CB1 receptor ligands and target compounds.

reported 2-aryl benzimidazoles derivatives with CB1 receptor affinity such as JM-14 and JM-21 (Fig. 1) [8]. The structure–activity relationship established on the basis of *in vitro* evaluation and the CoMFA modeling studies suggests two interesting regions to explore: the naphthalene ring and the pyridyl moiety [9].

In light of these results, we decide to design a new benzimidazole-based series structurally related to JM-21 and AM-679. The CoMFA analyses of the JM series suggest that in the naphthalene region, bulky groups or substitutions with electronegative atoms are favorable. Therefore, in the designed series, we retained the naphthalene, or incorporate a benzene ring substituted with electronegative substituents such as nitrile or nitro groups. Regarding the pyridine ring, electronegative groups next to the benzimidazole core are favorable for CB1 affinity. In order to exploit both, the electronic and steric requirements in this region, we replaced

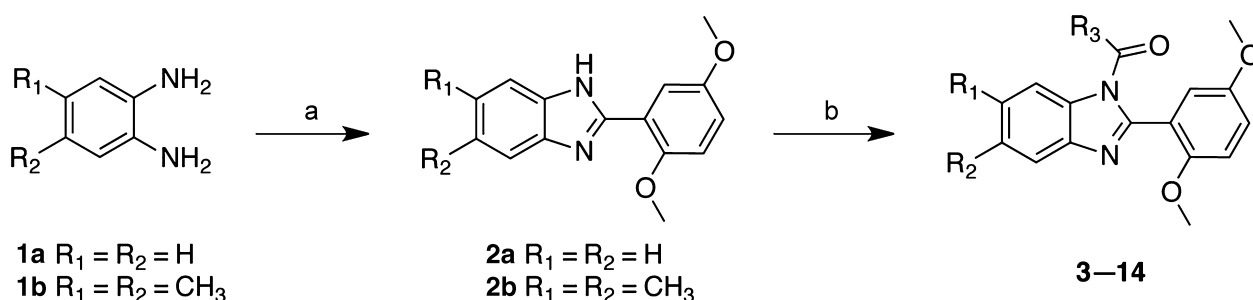
the pyridine in the previously reported series with a 2,5-dimethoxyphenyl substituent.

We report herein the synthesis, the CB1 receptor binding assays of a series of *N*-acyl-2,5-dimethoxyphenyl-1*H*-benzimidazoles and the molecular modeling of their putative binding modes.

Results and discussion

Chemistry

The general synthetic route for compounds 3–14 is outlined in Scheme 1. *N*-Aroyl-2,5-dimethoxyphenyl-1*H*-benzimidazole derivatives were obtained in two steps from the starting material *o*-phenylenediamines 1a,b, which were reacted with 2,5-dimethoxybenzaldehyde in ethanol yielding the corresponding benzimidazole derivatives 2a,b [10]. The obtained



Scheme 1. Reagents and conditions: (a) 2,5-dimethoxybenzaldehyde, ethanol, reflux, 24 h; (b) aromatic acyl chlorides, THF, Na₂CO₃, reflux, overnight.

Table 1. Synthesized target compounds and human CB1 receptor binding affinities for derivatives 3–10.

Compound	R ₁	R ₂	R ₃	Human CB1 K _i (nM) ^{a),b)}
3	H	H	1-naphtyl	3.5
4	H	H	2-naphtyl	25.0
5	H	H	3-nitrophenyl	1.2
6	H	H	4-cyanophenyl	8.0
7	CH ₃	CH ₃	1-naphtyl	16.0
8	CH ₃	CH ₃	4-nitrophenyl	6.0
9	CH ₃	CH ₃	3-nitrophenyl	3.9
10	CH ₃	CH ₃	4-cyanophenyl	5.0
11	CH ₃	CH ₃	2-naphtyl	NT ^{c)}
12	CH ₃	CH ₃	3-cyanophenyl	NT ^{c)}
13	H	H	4-nitrophenyl	NT ^{c)}
14	H	H	3-cyanophenyl	NT ^{c)}
CP55,940				0.6 ^{d)}

^{a)}Values are means of three experiments performed in triplicate.

^{b)}SD values were never higher than 10%.e.

^{c)}Non tested.

^{d)}According to kit manufacturer.

benzimidazoles were finally acylated under anhydrous conditions and inert atmosphere to yield the target compounds 3–14.

Human CB1 receptor affinity

The synthesized target compounds 3–10 were evaluated for their human CB1 receptor affinity and the results are summarized in Table 1. All the tested compounds showed binding affinity values in the nanomolar range. As a whole, the best affinity values ($K_i \leq 10$ nM) were observed for derivatives bearing electronegative groups in the aryl region. On one hand, compounds substituted in R₃ with a 3-nitrophenyl moiety showed the best binding affinity values regardless whether the R₁ and R₂ substitution pattern is hydrogen or a methyl group. On the other hand, the

1-naphtyl substitution at R₃ was better than that of 2-naphtyl moiety, as can be seen when comparing derivatives 3 and 4.

Molecular modeling of ligand CB1 interactions

Molecular docking calculations of the active ligands were performed using the CB1 receptor model previously reported by our group [9]. The main binding site has a volume of 506.25 Å³ and is defined by the extracellular side of transmembrane helices (TMH) 2, 3, 5, 6 and 7 of the receptor (Fig. 2A). Compound CP55,940 predicted binding mode resembles to that previously reported by other groups where the phenolic OH groups contact with K3.28(192) and the southern aliphatic hydroxyl (SAH) group points towards the solvent where it forms an H-bond interaction with D6.58(366) while the northern

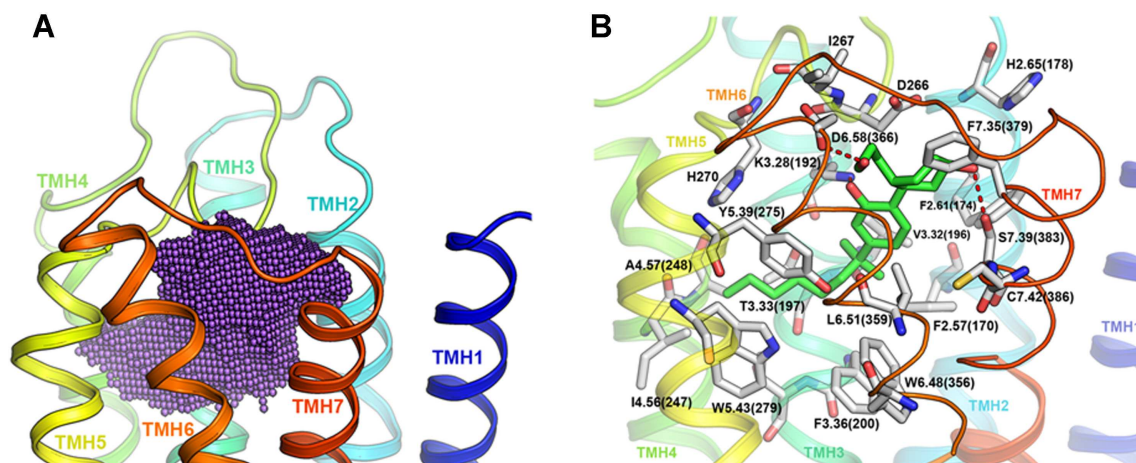


Figure 2. (A) Schematic representation of CB1 receptor model binding site, the volume of the calculated cavity represented as purple spheres is ~ 500 Å³. (B) FRED predicted binding mode for CP55,940 and its predicted intermolecular interactions with the CB1 receptor.

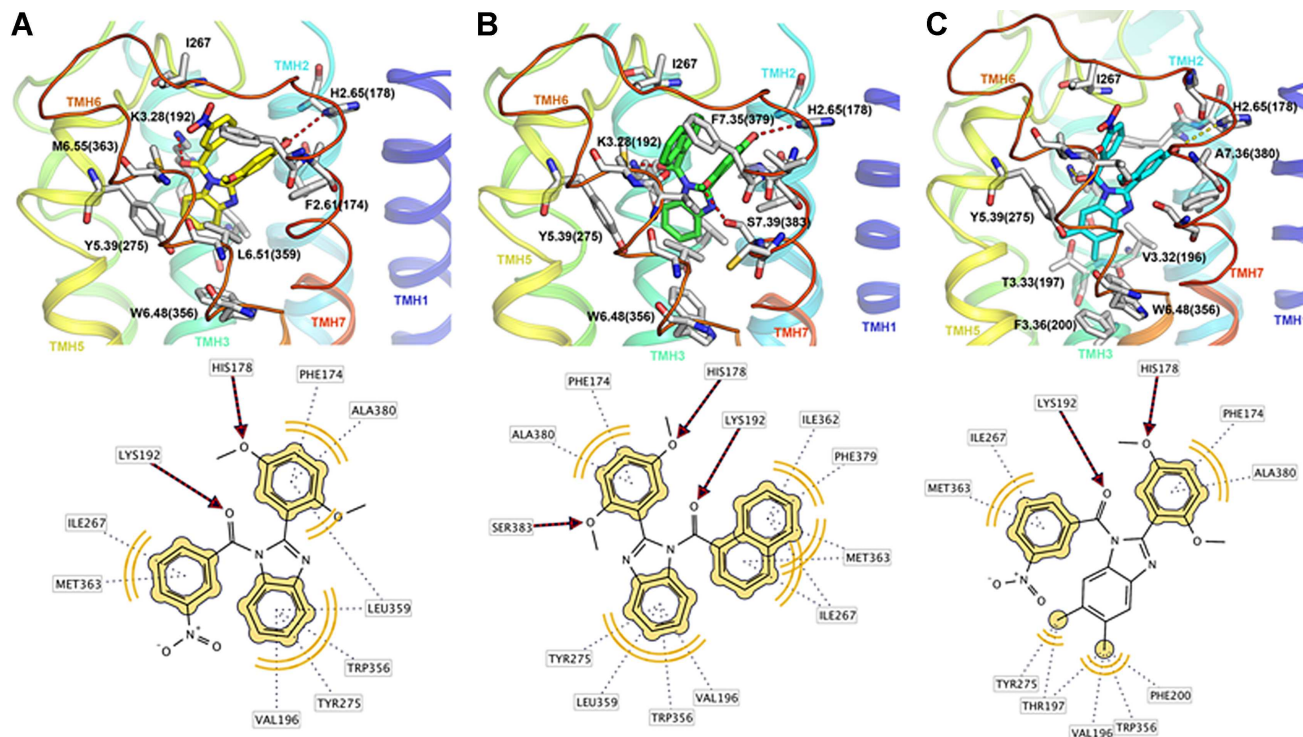


Figure 3. FRED predicted binding mode and 2D schematic diagrams for the protein-ligand interactions of the CB1 receptor with derivatives 5 (A), 3 (B) and 9 (C).

aliphatic hydroxyl (NAH) binds to S7.39(383), and the C3 alkyl chain of the ligand was positioned toward TM5 (Fig. 2B) [11].

Our docking results reveal that all active compounds present a similar binding mode pattern, with benzimidazole moieties getting deep into the pocket delimited by TMH 3–4–5–6 region of CB1, which has been reported to be the binding region of the structurally related cannabimimetic indoles ligands [12]. As shown in Fig. 3, the most active compounds display similar interactions with an aromatic cluster composed by residues F3.36(200), Y5.39(275), W5.43(279) and W6.48 (356), involved in CB1 receptor activation (W6.48/F3.36 ‘toggle switch’) [13].

Because of the high homology of CB1 and CB2 receptor in the predicted binding mode region of our derivatives (6 Å from center of mass of all docked ligands, 65.8% identity and 86.8% sequence similarity) it is plausible that the compounds might also bind to CB2 receptors. For the related indole CB1 ligands, increasing the N-alkyl substituent carbon chain length had little influence on CB1 binding but affinity for CB2 increases [14]. When substituted with methyl groups at R₂ and R₃, the compounds bind deeper in the site and establish aliphatic interaction with V3.32(196) and T3.33(197). The 5-methoxy group establishes an H-bond interaction with H2.65(178) and aliphatic interaction with the side chains of F2.61(174) and A7.36(280). An additional hydrogen bond interaction could be established between the 2-methoxy substituent group of derivative 3 and the side-chain of S7.39(383). In all cases, the

central ketone formed a hydrogen bond with K3.28(192). The aroyl group activity is favored if the nitro substitution is in position 3 or the naphthyl group substituted at position 1, where both moieties have aliphatic contacts with the side chains of I267 at the extracellular loop 2 and M6.55(363). This binding mode is similar to our previously reported binding

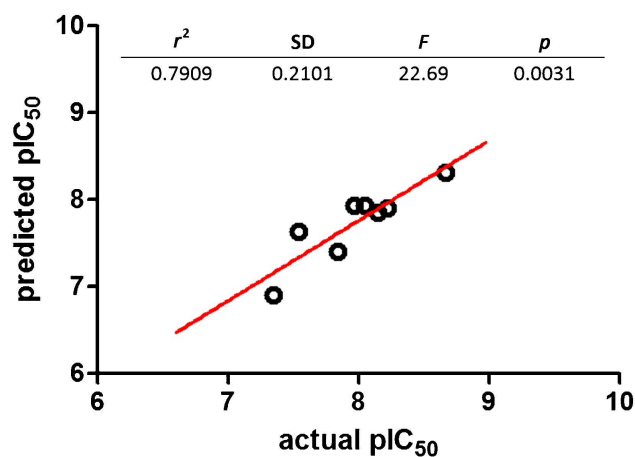


Figure 4. Experimental versus predicted pIC₅₀ values. r^2 = linear regression coefficient, SD = standard deviation, F = the F-test value, p = statistical significance.

Table 2. Experimental and predicted pIC₅₀ values for derivatives 3–10.

Compound number	Experimental pIC ₅₀	Predicted pIC ₅₀
3	8.2218	7.9030
4	7.3468	6.9039
5	8.6692	8.3138
6	7.8416	7.4021
7	7.5406	7.6327
8	7.9666	7.9350
9	8.1459	7.8533
10	8.0458	7.9286

modes for aminoalkylindoles and WIN55,212 aroyl-up conformation reported by Shim and co-workers [15].

Validation of CoMFA-based design

A high correlation between CoMFA-predicted and experimental affinities was observed. As can be seen in the experimental versus predicted pIC₅₀ graphic (Fig. 4A), the homogenous linear distribution of the affinity values, high r^2 value, small standard deviation and statistical significance validate the model robustness. The experimental versus CoMFA-predicted pIC₅₀ values of the active compounds are resumed in Table 2.

Conclusion

Based on a previously developed CoMFA model and biological evaluation, we designed and synthesized a series of novel benzimidazole derivatives with a 2,5-dimethoxyphenyl moiety targeting the CB1 receptor. Subsequent binding affinity evaluation revealed that 8 out of 12 compounds displayed high binding affinity for the human CB1 receptor with K_i values in the nanomolar range, and comparable to the well-known CB1 ligand CP55,940. Molecular modeling binding mode of the promising compound 5 revealed a similar binding mode to that observed for the compounds used to build the CoMFA model. These results and the external validation of the 3D-QSAR provided additional information for further design efforts. Finally, considering the importance of evaluating selectivity CB1/CB2 as a complement to address the full therapeutic scope of these compounds, further experiments to establish selectivity towards CB2 receptor will be performed in forthcoming work and will be reported in the near future.

Experimental

Chemistry

All organic solvents used for the syntheses were analytical grade. Melting points were determined on a Stuart Scientific SMP3 apparatus and are uncorrected. IR spectra were

recorded on a Bruker Vector 22 spectrophotometer using KBr discs. ¹H and ¹³C NMR spectra were obtained on a Bruker AM-400 spectrometer. The chemical shifts are expressed in ppm (δ scale) downfield from TMS, J values are given in Hertz for solutions in CDCl₃ unless otherwise indicated. Column chromatography was performed on Merck silica gel 60 (70–230 mesh). Thin layer chromatographic separations were performed on Merck silica gel 60 (70–230 mesh) chromatofolios. Purity of all final derivatives for biological testing was confirmed to be >95% as determined using elemental analysis carried out on a FISON EA 1108 CHNS-O analyzer.

General procedure for the synthesis of (2-(2,5-dimethoxyphenyl)-1H-benzo[d]imidazol-1-yl)-(aryl)methanone derivatives

A solution of respective aromatic acyl chloride (1.5 equiv.) in anhydrous THF (20 mL) containing Na₂CO₃ (2 equiv.) and the corresponding 2-(2,5-dimethoxyphenyl)-1H-benzo[d]imidazole derivative (1 equiv.) is heated under reflux overnight. The reaction mixture is then filtered and the solvent removed under vacuum. The obtained crude is then purified by chromatography using methylene chloride as mobile phase.

(2-(2,5-Dimethoxyphenyl)-1H-benzo[d]imidazol-1-yl)-(naphthalen-1-yl)methanone (3)

Light brown solid, yield = 36%; mp: 187–189°C; IR (KBr) cm⁻¹: 1717 (C=O); ¹H NMR (400 MHz, CDCl₃) δ 8.26 (d, J = 7.6 Hz, 1H, H2''), 7.85 (m, 3H, H4'', H5'', H8''), 7.62 (d, J = 5.8 Hz, 1H, H3''), 7.60–7.44 (m, 3H, H6, H6'', H7''), 7.36 (t, J = 6.4 Hz, 1H, H5), 7.28 (d, J = 6.4 Hz, 2H, H4, H7), 7.04 (s, 1H, H6'), 6.64 (d, J = 8.5 Hz, 1H, H4'), 6.31 (d, J = 8.5 Hz, 1H, H3'), 3.69 (s, 3H, OCH₃), 3.40 (s, 3H, OCH₃). ¹³C NMR (101 MHz, CDCl₃) δ 168.8, 153.8, 151.9, 150.6, 143.3, 134.7, 133.9, 133.8, 131.3, 131.0, 130.4, 128.9, 128.3, 126.9, 125.4, 125.3, 124.7, 124.34, 121.2, 120.6, 117.8, 115.6, 114.3, 111.7, 56.2, 56.0. Anal. Elem. Calcd. C: 76.45, H: 4.94, N: 6.86. Found. C: 76.18, H: 5.02, N: 6.79.

(2-(2,5-Dimethoxyphenyl)-1H-benzo[d]imidazol-1-yl)-(naphthalen-2-yl)methanone (4)

White solid, yield = 54%; mp: 227–229°C; IR (KBr) cm⁻¹: 1710 (C=O); ¹H NMR (400 MHz, CDCl₃) δ 8.21 (s, 1H, H2''), 7.94–7.83 (m, 4H, H3'', H6'', H7'', H8''), 7.80 (d, J = 8.1 Hz, 1H, H4), 7.61 (t, J = 7.4 Hz, 1H, H4''), 7.52 (t, J = 7.4 Hz, 1H, H5''), 7.43 (s, 1H, H6'), 7.34 (m, 2H, H5, H6), 7.23 (m, 1H, H7), 6.71 (d, J = 8.9 Hz, 1H, H4'), 6.48 (d, J = 8.9 Hz, 1H, H3'), 3.78 (s, 3H, OCH₃), 3.41 (s, 3H, OCH₃). ¹³C NMR (101 MHz, CDCl₃) δ 169.0, 154.2, 151.8, 150.3, 143.18, 135.9, 135.0, 133.2, 132.3, 130.2, 129.7, 129.4, 128.7, 128.2, 127.4, 125.9, 124.8, 124.3, 120.9, 120.5, 118.0, 116.0, 113.5, 112.0, 56.3, 55.5. Anal. Elem. Calcd. C: 76.45, H: 4.94, N: 6.86. Found. C: 76.22, H: 4.99, N: 6.81.

(2-(2,5-Dimethoxyphenyl)-1H-benzo[d]imidazol-1-yl)(3-nitrophenyl)methanone (5)

Yellow solid, yield = 51%; mp: 152–154°C; IR (KBr) cm⁻¹: 1709 (C=O); ¹H NMR (400 MHz, CDCl₃) δ 8.38 (s, 1H, H2''), 8.23 (dd,

$J = 8.2, 1.1 \text{ Hz}$, 1H, H4''), 7.96 (d, $J = 8.0 \text{ Hz}$, 1H, H6''), 7.89 (d, $J = 7.1 \text{ Hz}$, 1H, H4), 7.78 (d, $J = 7.2 \text{ Hz}$, 1H, H7), 7.49 (t, $J = 8.0 \text{ Hz}$, 1H, H5''), 7.41 (m, 2H, H5, H6), 7.33 (d, $J = 3.1 \text{ Hz}$, 1H, H6'), 6.75 (dd, $J = 9.0, 3.1 \text{ Hz}$, 1H, H4'), 6.39 (d, $J = 9.0 \text{ Hz}$, 1H, H3'), 3.79 (s, 3H, OCH₃), 3.50 (s, 3H, OCH₃). ¹³C NMR (101 MHz, CDCl₃) δ 167.0, 154.4, 150.8, 150.0, 147.7, 143.1, 135.6, 134.9, 134.6, 129.4, 127.6, 125.8, 125.5, 125.2, 120.7, 119.0, 115.6, 114.0, 112.0, 56.3, 55.7. Anal. Elem. Calcd. C: 65.50, H: 4.25, N: 10.42. Found. C: 65.06, H: 4.48, N: 10.11.

(2-(2,5-Dimethoxyphenyl)-1H-benzo[d]imidazol-1-yl)(4-cyanophenyl)methanone (6)

White solid, yield = 66%; mp: 158–161°C; IR (KBr) cm⁻¹: 1720 (C=O); ¹H NMR (400 MHz, CDCl₃) δ 7.95–7.80 (m, 3H, H4, H2'', H6''), 7.67 (m, 2H, H3'', H5''), 7.39 (m, 4H, H5, H6, H7, H6'), 6.81 (dd, $J = 9.0, 2.9 \text{ Hz}$, 1H, H4'), 6.47 (d, $J = 9.0 \text{ Hz}$, 1H, H3'), 3.84 (s, 3H, OCH₃), 3.50 (s, 3H, OCH₃). ¹³C NMR (101 MHz, CDCl₃) δ 167.1, 154.5, 150.9, 150.1, 143.2, 136.3, 134.6, 134.5, 134.2, 134.1, 129.3, 125.6, 125.1, 120.7, 118.9, 117.7, 115.6, 113.8, 112.8, 112.2, 56.4, 55.7. Anal. Elem. Calcd. C: 72.05, H: 4.47, N: 10.96. Found. C: 71.88, H: 4.61, N: 10.02.

(2-(2,5-Dimethoxyphenyl)-5,6-dimethyl-1H-benzo[d]imidazol-1-yl)(naphthalen-1-yl)methanone (7)

White solid, yield = 29%; mp: 176–178°C; IR (KBr) cm⁻¹: 1704 (C=O); ¹H NMR (400 MHz, CDCl₃) δ 8.18 (d, $J = 7.9 \text{ Hz}$, 1H, H2''), 7.81 (m, 2H, H4'', H8''), 7.65–7.42 (m, 5H, H4, H7, H5'', H6'', H7''), 7.26 (t, $J = 7.9 \text{ Hz}$, 1H, H3''), 6.92 (d, $J = 3.0 \text{ Hz}$, 1H, H6'), 6.58 (dd, $J = 9.0, 3.1 \text{ Hz}$, 1H, H4'), 6.24 (d, $J = 9.0 \text{ Hz}$, 1H, H3'), 3.65 (s, 3H, OCH₃), 3.39 (s, 3H, OCH₃), 2.40 (s, 3H, CH₃), 2.33 (s, 3H, CH₃). ¹³C NMR (101 MHz, CDCl₃) δ 169.0, 153.6, 151.0, 150.6, 141.8, 134.6, 133.7, 133.5, 133.1, 131.3, 130.8, 128.8, 128.1, 126.8, 125.4, 124.3, 121.4, 120.6, 117.6, 115.3, 114.8, 111.5, 56.2, 56.0, 21.0, 20.7. Anal. Elem. Calcd. C: 77.04, H: 5.54, N: 6.42. Found. C: 76.94, H: 5.58, N: 6.35.

(2-(2,5-Dimethoxyphenyl)-5,6-dimethyl-1H-benzo[d]imidazol-1-yl)(4-nitrophenyl)methanone (8)

Yellow solid, yield = 78%; mp: 172–174°C; IR (KBr) cm⁻¹: 1710 (C=O); ¹H NMR (400 MHz, CDCl₃) δ 8.11 (d, $J = 8.7 \text{ Hz}$, 2H, H2'', H6''), 7.77 (d, $J = 8.7 \text{ Hz}$, 2H, H3'', H5''), 7.62 (s, 1H, H4), 7.43 (s, 1H, H7), 7.31 (d, $J = 3.0 \text{ Hz}$, 1H, H6'), 6.77 (dd, $J = 9.0, 3.1 \text{ Hz}$, 1H, H4'), 6.43 (d, $J = 9.0 \text{ Hz}$, 1H, H3'), 3.80 (s, 3H, OCH₃), 3.48 (s, 3H, OCH₃), 2.40 (s, 3H, CH₃), 2.36 (s, 3H, CH₃). ¹³C NMR (101 MHz, CDCl₃) δ 167.4, 154.4, 150.3, 150.1, 141.7, 139.0, 135.0, 134.1, 133.0, 131.4, 123.3, 120.8, 118.1, 116.1, 114.1, 112.2, 56.4, 55.7, 21.1, 20.7. Anal. Elem. Calcd. C: 66.81, H: 4.91, N: 9.74. Found. C: 66.58, H: 5.03, N: 9.45.

(2-(2,5-Dimethoxyphenyl)-5,6-dimethyl-1H-benzo[d]imidazol-1-yl)(3-nitrophenyl)methanone (9)

Ligth yellow solid, yield = 61%; mp: 191–193°C; IR (KBr) cm⁻¹: 1710 (C=O); ¹H NMR (400 MHz, CDCl₃) δ 8.34 (s, 1H, H2''), 8.20 (d, $J = 8.0 \text{ Hz}$, 1H, H4''), 7.93 (d, $J = 7.6 \text{ Hz}$, 1H, H6''), 7.62 (d, $J = 3.5 \text{ Hz}$, 2H, H4, H7), 7.45 (t, $J = 7.6 \text{ Hz}$, 1H, H5''), 7.29 (d, $J = 2.9 \text{ Hz}$, 1H, H6'), 6.71 (dd, $J = 9.0, 2.9 \text{ Hz}$, 1H, H4'), 6.35 (d,

$J = 9.0 \text{ Hz}$, 1H, H3'), 3.78 (s, 3H, OCH₃), 3.49 (s, 3H, OCH₃), 2.40 (d, $J = 8.4 \text{ Hz}$, 6H, 2 x CH₃). ¹³C NMR (101 MHz, CDCl₃) δ 167.1, 154.3, 150.0, 149.9, 147.5, 141.7, 135.6, 135.1, 134.2, 133.1, 129.3, 127.4, 125.4, 121.1, 120.7, 118.7, 115.5, 114.33, 112.0, 56.3, 55.7, 21.0, 20.7. Anal. Elem. Calcd. C: 66.81, H: 4.91, N: 9.74. Found. C: 66.63, H: 4.99, N: 9.62.

(2-(2,5-Dimethoxyphenyl)-5,6-dimethyl-1H-benzo[d]imidazol-1-yl)(4-cyanophenyl)methanone (10)

White solid; yield = 49%; mp: 143–145°C; IR (KBr) cm⁻¹: 1703 (C=O); ¹H NMR (400 MHz, CDCl₃) δ 7.71 (d, $J = 8.4 \text{ Hz}$, 2H, H2'', H6''), 7.61 (s, 1H, H4), 7.56 (d, $J = 8.4 \text{ Hz}$, 2H, H3'', H5''), 7.41 (s, 1H, H7), 7.30 (d, $J = 3.1 \text{ Hz}$, 1H, H6'), 6.80 (dd, $J = 9.0, 3.1 \text{ Hz}$, 1H, H4'), 6.44 (d, $J = 9.0 \text{ Hz}$, 1H, H3'), 3.81 (s, 3H, OCH₃), 3.47 (s, 3H, OCH₃), 2.40 (s, 3H, CH₃), 2.36 (s, 3H, CH₃). ¹³C NMR (101 MHz, CDCl₃) δ 167.7, 154.4, 150.1, 150.0, 141.7, 137.4, 134.9, 134.0, 133.0, 131.9, 130.8, 121.0, 120.7, 118.1, 116.6, 116.1, 114.1, 112.2, 56.4, 55.7, 21.0, 20.7. Anal. Elem. Calcd. C: 72.98, H: 5.14, N: 10.21. Found. C: 72.74, H: 5.49, N: 10.00.

(2-(2,5-Dimethoxyphenyl)-5,6-dimethyl-1H-benzo[d]imidazol-1-yl)(naphthalen-2-yl)methanone (11)

White solid, yield = 25%; mp: 193–195°C; IR (KBr) cm⁻¹: 1702 (C=O); ¹H NMR (400 MHz, CDCl₃) δ 8.14 (s, 1H, H2''), 7.84 (d, $J = 8.5 \text{ Hz}$, 1H, H8''), 7.82 (s, 2H, H7'', H6''), 7.78 (d, $J = 8.1 \text{ Hz}$, 1H, H3''), 7.63 (s, 1H, H4), 7.60 (t, $J = 7.1 \text{ Hz}$, 1H, H5''), 7.51 (t, $J = 7.1 \text{ Hz}$, 1H, H4''), 7.38 (d, $J = 3.1 \text{ Hz}$, 1H, H6'), 7.22 (s, 1H, H7), 6.65 (dd, $J = 9.0, 3.1 \text{ Hz}$, 1H, H4'), 6.41 (d, $J = 9.0 \text{ Hz}$, 1H, H3'), 3.76 (s, 3H, OCH₃), 3.41 (s, 3H, OCH₃), 2.39 (s, 3H, CH₃), 2.28 (s, 3H, CH₃). ¹³C NMR (101 MHz, CDCl₃) δ 169.2, 154.2, 150.9, 150.2, 141.7, 135.8, 134.2, 133.5, 133.3, 133.1, 132.2, 130.4, 129.6, 129.2, 128.5, 128.2, 127.3, 125.9, 121.3, 120.5, 117.7, 115.8, 113.9, 111.9, 56.3, 55.5, 21.0, 20.7. Anal. Elem. Calcd. C: 77.04, H: 5.54, N: 6.42. Found. C: 76.70, H: 5.71, N: 6.19.

(2-(2,5-Dimethoxyphenyl)-5,6-dimethyl-1H-benzo[d]imidazol-1-yl)(3-cyanophenyl)methanone (12)

White solid, yield = 52%; mp: 190–192°C; IR (KBr) cm⁻¹: 1704 (C=O); ¹H NMR (400 MHz, CDCl₃) δ 7.86 (s, 1H, H2''), 7.82 (d, $J = 7.9 \text{ Hz}$, 1H, H4''), 7.66 (d, $J = 7.8 \text{ Hz}$, 1H, H6''), 7.62 (s, 1H, H4), 7.50 (s, 1H, H7), 7.39 (t, $J = 7.8 \text{ Hz}$, 1H, H5''), 7.29 (d, $J = 3.0 \text{ Hz}$, 1H, H6'), 6.78 (dd, $J = 9.0, 3.1 \text{ Hz}$, 1H, H4'), 6.43 (d, $J = 9.0 \text{ Hz}$, 1H, H3'), 3.83 (s, 3H, OCH₃), 3.49 (s, 3H, OCH₃), 2.39 (d, $J = 12.3 \text{ Hz}$, 6H, 2 x CH₃). ¹³C NMR (101 MHz, CDCl₃) δ 167.2, 154.5, 150.08, 150.0, 141.7, 137.0, 135.0, 134.7, 134.1, 134.0, 133.0, 129.1, 121.1, 120.7, 118.6, 117.8, 115.5, 114.2, 112.6, 112.2. Anal. Elem. Calcd. C: 72.98, H: 5.14, N: 10.21. Found. C: 72.68, H: 5.44, N: 9.89.

(2-(2,5-Dimethoxyphenyl)-1H-benzo[d]imidazol-1-yl)(4-nitrophenyl)methanone (13)

Yellow solid, yield = 75%; mp: 132–133°C; IR (KBr) cm⁻¹: 1705 (C=O); ¹H NMR (400 MHz, CDCl₃) δ 8.14 (d, $J = 8.8 \text{ Hz}$, 2H, H2'', H6''), 7.88 (d, $J = 7.7 \text{ Hz}$, 1H, H4), 7.82 (d, $J = 8.8 \text{ Hz}$, 2H, H3'',

H5"), 7.57 (d, $J=8.0$ Hz, 1H, H7), 7.41 (td, $J=7.7, 1.1$ Hz, 1H, H6), 7.38–7.32 (m, 2H, H5, H6"), 6.81 (dd, $J=9.0, 3.1$ Hz, 1H, H4'), 6.48 (d, $J=9.0$ Hz, 1H, H3'), 3.82 (s, 3H, OCH₃), 3.50 (s, 3H, OCH₃). ¹³C NMR (101 MHz, CDCl₃) δ 167.3, 154.5, 150.1, 143.1, 138.7, 134.5, 131.4, 125.6, 125.1, 123.4, 120.7, 118.4, 116.2, 113.7, 112.2, 56.4, 55.7. Anal. Elem. Calcd. C: 65.50, H: 4.25, N: 10.42. Found. C: 65.10, H: 4.42, N: 10.35.

(2-(2,5-Dimethoxyphenyl)-1H-benzo[d]imidazol-1-yl)(3-cyanophenyl)methanone (**14**)

White solid, yield = 41%; mp: 138–140°C; IR (KBr) cm⁻¹: 1720 (C=O); ¹H NMR (400 MHz, CDCl₃) δ 8.17–7.08 (m, 9H, H4, H5, H6, H7, H6', H2", H4", H5", H6"), 6.83 (s, 1H, H4'), 6.49 (s, 1H, H3'), 3.82 (s, 3H, OCH₃), 3.47 (s, 3H, OCH₃). ¹³C NMR (101 MHz, CDCl₃) δ 167.5, 154.5, 150.9, 150.1, 143.2, 137.1, 134.6, 132.1, 130.9, 125.5, 125.0, 120.7, 118.4, 116.8, 116.1, 113.7, 112.2, 56.4, 55.6. Anal. Elem. Calcd. C: 72.05, H: 4.47, N: 10.96. Found. C: 71.74, H: 4.63, N: 10.09.

CB1 receptor binding assays

Competition binding assays were performed with [³H]CP-55,940 ($K_d=0.60$ nM, Perkin Elmer, USA) as the labeled ligand in membrane preparation of CB1 receptor (Perkin Elmer Product No.: 6110129400UA, Lot No.: 509–845-A). All ligands were diluted in assay buffer containing 20 mM Hepes pH 7.4, 5 mM MgCl₂, 1 mM EDTA and 0.3% BSA. All the new synthesized compounds were first subjected to a preliminary screening using three concentrations (1, 0.1 and 0.01 μ M). Assay solutions were incubated for 60 min at 30°C, with a final assay volume of 550 μ L and a final membrane concentration of 10 μ g/ μ L. Compounds which displaced [³H]CP55,940 by more than 50% at 1 μ M were further analyzed. Displacement curves were generated by incubating with 0.5 nM of [³H]CP55,940. For competition binding assays, IC₅₀ values were determined by nonlinear regression using GraphPad Prism v.5 (GraphPad Software, Inc., USA). K_i values were then calculated using the Cheng-Prusoff equation based on K_d v/s IC₅₀ values obtained from saturation binding analyses [16].

Molecular modeling of ligand CB1 interactions

All ligands were constructed using MarvinSketch v6.2 (ChemAxon Ltd., Hungary). Multiple conformer database of the ligands was prepared with OMEGA v2.5.1.4 (OpenEye Scientific Software, Santa Fe, NM) [17]. The AM1BCC charges for ligands and AmberFF99sb for protein were assigned using QUACPAC v1.6.3.1 (OpenEye Scientific Software, Santa Fe, NM), the receptor binding sites prepared with Make_Receptor GUI and docking calculations performed using FRED v3.0.1 (OpenEye Scientific Software, Santa Fe, NM) with the ChemGauss4 scoring function [18]. A set of 10 solutions for each ligand was obtained and the best binding mode selected according to the consensus score protocol (with LigScore, Jain, PMF and Ludi 1–3 scoring functions) available with Discovery Studio v2.1 (Accelrys Inc., San Diego) was energy minimized using the conjugate gradient algorithm until a RMS gradient of 0.001 kcal/molÅ was reached. The side-chain of residues

neighboring 6 Å from the center of mass of ligand position were considered flexible during local minimization. The CHARMM22 force field with a dielectric constant of 4 and a distance-dependent dielectric implicit solvent model to mimic the membrane environment was employed [19]. Two-dimensional protein-ligand interaction schemes were obtained with LigandScout v3.12 (Inte:Ligand GmbH, Austria).

Supported by Chilean Commission for Scientific Research and Technology CONICYT grants FONDECYT N°1100493 to C.D.P.-M. and FONDECYT INICIO N°11130701 to J.M.-R. C.E.-B. is a CONICYT-CHILE PhD fellow. C.D.P. acknowledges the Pontificia Universidad Católica de Chile for grant VRI/2014. C.F.L. acknowledges OpenEye Scientific Software, ChemAxon and Inte:Ligand for academic licenses of their products.

The authors have declared no conflict of interest.

References

- [1] R. Mechoulam, J. J. Feigenbaum, *Prog. Med. Chem.* **1987**, *24*, 159–207.
- [2] a) D. Piomelli, *Curr. Opin. Investig. Drugs* **2005**, *6*, 672–679. b) D. M. Lambert, C. J. Fowler, *J. Med. Chem.* **2005**, *48*, 5059–5087. c) S. Pisanti, P. Picardi, A. D'Alessandro, C. Laezza, M. Bifulco, *Trends Pharmacol. Sci.* **2013**, *34*, 273–282.
- [3] N. Lambeng, F. Lebon, B. Christophe, M. Burton, M. De Ryck, L. Quéré, *Bioorg. Med. Chem. Lett.* **2007**, *17*, 272–277.
- [4] S. Munro, K. L. Thomas, M. Abu-Shaar, *Nature* **1993**, *365*, 61–65.
- [5] R. G. Pertwee, A. Thomas, Ed. *Humana Press* (Ed.: P. H. Reggio), **2009**, pp. 361–392.
- [6] J. H. M. Lange, C. G. Kruse, *Chem. Rec.* **2008**, *8*, 156–168.
- [7] S. L. Palmer, G. A. Thakur, A. Makriyannis, *Chem. Phys. Lipids* **2002**, *121*, 3–19.
- [8] a) C. Manera, T. Tuccinardi, A. Martinelli, *Mini-Rev. Med. Chem.* **2008**, *8*, 370–387. b) J. W. Huffman, L. W. Padgett, *Curr. Med. Chem.* **2005**, *12*, 1395–1411.
- [9] J. A. Mella-Raipan, C. F. Lagos, G. Recabarren-Gajardo, C. Espinosa-Bustos, J. Romero-Parra, H. Pessoa-Mahana, P. Iturriaga-Vasquez, C. D. Pessoa-Mahana, *Molecules* **2013**, *18*, 3972–4001.
- [10] C. D. Pessoa-Mahana, A. Nuñez, C. Espinosa, J. Mella-Raipan, H. Pessoa-Mahana, *J. Braz. Chem. Soc.* **2010**, *21*, 63–70.
- [11] a) J. Y. Shim, W. J. Welsh, A. C. Howlett, *Biopolymers* **2003**, *71*, 169–189. b) O. M. Salo, M. Lahtela-Kakkonen, J. Gynther, T. Jarvinen, A. Poso, *J. Med. Chem.* **2004**, *47*, 3048–3057. c) A. Kapur, D. P. Hurst, D. Fleischer, R. Whitnell, G. A. Thakur, A. Makriyannis, P. H. Reggio, M. E. Abood, *Mol. Pharmacol.* **2007**, *71*, 1512–1524. d) J.-Y. Shim, L. Padgett, *Methods in Enzymology*, Academic Press, **2013**, pp. 337–355.

- [12] J. W. Huffman, R. Mabon, M.-J. Wu, J. Lu, R. Hart, D. P. Hurst, P. H. Reggio, J. L. Wiley, B. R. Martin, *Bioorg. Med. Chem.* **2003**, *11*, 539–549.
- [13] R. Singh, D. P. Hurst, J. Barnett-Norris, D. L. Lynch, P. H. Reggio, F. Guarnieri, *J. Pept. Res.* **2002**, *60*, 357–370.
- [14] M. M. Aung, G. Griffin, J. W. Huffman, M.-J. Wu, C. Keel, B. Yang, V. M. Showalter, M. E. Abood, B. R. Martin, *Drug Alcohol Depend.* **2000**, *60*, 133–140.
- [15] a) A. Gonzalez, L. S. Duran, R. Araya-Secchi, J. A. Garate, C. D. Pessoa-Mahana, C. F. Lagos, T. Perez-Acle, *Bioorg. Med. Chem.* **2008**, *16*, 4378–4389. b) J. Y. Shim, A. C. Howlett, *J. Chem. Inf. Model.* **2006**, *46*, 1286–1300.
- [16] Y. Cheng, W. H. Prusoff, *Biochem. Pharmacol.* **1973**, *22*, 3099–3108.
- [17] a) P. C. Hawkins, A. G. Skillman, G. L. Warren, B. A. Ellington, M. T. Stahl, *J. Chem. Inf. Model.* **2010**, *50*, 572–584. b) OMEGA, v2.5.1.4: OpenEye Scientific Software, Santa Fe, NM. (<http://www.eyesopen.com>).
- [18] a) A. Jakalian, D. B. Jack, C. I. Bayly, *J. Comput. Chem.* **2002**, *23*, 1623–1641. b) QUACPAC, v1.6.3.1: OpenEye Scientific Software, Santa Fe, NM. (<http://www.eyesopen.com>). c) FRED, v3.0.1: OpenEye Scientific Software, Santa Fe, NM. (<http://www.eyesopen.com>). d) M. McGann, *J. Comput. Aided Mol. Des.* **2012**, *26*, 897–906.
- [19] B. R. Brooks, C. L. Brooks, A. D. Mackerell, L. Nilsson, R. J. Petrella, B. Roux, Y. Won, G. Archontis, C. Bartels, S. Boresch, A. Caflisch, L. Caves, Q. Cui, A. R. Dinner, M. Feig, S. Fischer, J. Gao, M. Hodoscek, W. Im, K. Kuczera, T. Lazaridis, J. Ma, V. Ovchinnikov, E. Paci, R. W. Pastor, C. B. Post, J. Z. Pu, M. Schaefer, B. Tidor, R. M. Venable, H. L. Woodcock, X. Wu, W. Yang, D. M. York, M. Karplus, *J. Comput. Chem.* **2009**, *30*, 1545–1614.